International Journal of High-Rise Buildings
September 2013, Vol 2, No 3, 245-255

International Journal of
High-Rise Buildings
www.ctbuh-korea.org/ijhrb/index.php

Wind Load Combinations Including Torsion for Rectangular Medium-rise Buildings

T. Stathopoulos†, M. Elsharawy, and K. Galal

Faculty of Engineering and Computer Science, Concordia University, Montréal, Québec, Canada

Abstract

This paper presents the results of a set of wind tunnel tests carried out to examine wind-induced overall structural loads on rectangular medium-rise buildings. Emphasis was directed towards torsion and its correlation with peak shear forces in transverse and longitudinal directions. Two building models with the same horizontal dimensions but different gabled-roof angles (0^o and 45^o) were tested at different full-scale equivalent eave heights (20, 30, 40, 50, and 60 m) in open terrain exposure for all wind directions (every 15^o). Wind-induced pressures were integrated over building surfaces and results were obtained for along-wind force, across-wind force, and torsional moment. Maximum wind force component was given along with the other simultaneously-observed wind force components normalized by the overall peak. The study found that for flat-roofed buildings maximum torsion for winds in transverse direction is associated with 80% of the overall shear force perpendicular to the longer horizontal building dimension; and 45% of the maximum shear occurs perpendicular to the smaller horizontal building dimension. Comparison of the wind tunnel results with current torsion provisions in the American wind standard, the Canadian and European wind codes demonstrate significant discrepancies. Suggested load combination factors were introduced aiming at an adequate evaluation of wind load effects on rectangular medium-rise buildings.

Keywords: Wind loads, Load combinations, Torsion, Codes, Building design

1. Introduction

Adequate wind design of buildings depends on the success in predicting the actual effects of turbulent wind forces in order to account for the most critical design scenarios which may occur during a certain design period. Along-wind force fluctuations are generated to a large extent by approaching flow turbulence; but fluctuations in across-wind force and torsion are generally dominated by vortex shedding causing asymmetric pressure distributions around building envelopes (Tamura et al., 2003). During the past decades, much has been learned about the variation of local wind pressures on building cladding and the total effective wind forces (along- and across-wind) on the main structural building systems of medium-rise buildings (Stathopoulos & Dumitrescu, 1989, Sanni et al., 1992). Recently, Elsharawy et al. (2012) found significant discrepancies among the current wind codes and standards in evaluating wind-induced torsion on medium-rise buildings. Furthermore, a study by Elsharawy et al. (2013) shows a significant difference between Canadian wind load provisions and the wind tunnel measurements in evaluating the critical torsion on medium-rise buildings with different roof slopes (0^o and 45^o). On the other hand, peak torsion and its correlation with peak along- and across-wind forces are of utmost importance for adequate building design. Wind load combinations (i.e., along-wind force associated with across-wind forces and vice versa) for medium-rise buildings, defined by ASCE 7-10 as having height less than 60 m but greater than 18 m with lowest natural frequency > 1 Hz, have been simplified by applying 0.75 of the full wind loads in both along- and across-wind directions simultaneously (ASCE 7-10, NBCC 2010). In another load combination case including torsion, ASCE 7-10 requires applying 0.563 of the full wind loads with an equivalent eccentricity equal to 15% of the facing building horizontal dimension in both along- and across-wind directions simultaneously. However, a similar torsional load case in NBCC 2010 applies 0.75 of the full wind load on half of building face and 0.38 of the full wind load in both along- and across-wind directions on the other half simultaneously. Tamura et al. (2008) and Keast et al. (2012) studied wind load combinations including torsion for medium-rise buildings. The first study shows the importance of considering the wind load combinations on the peak normal stress generated in the building columns. Based on testing of a limited number of building models, the latter study concludes that for rectangular buildings the peak overall torsion occurs simultaneously with 30~40% of the peak overall drag force. Additional experimental results for testing different building configurations are still required to confirm and generalize these results.

†Corresponding author: Ted Stathopoulos
Tel: +1-514-848-2424; Fax: +1-514-848-7965
E-mail: statho@bcee.concordia.ca

The current study reports the analysis and code comparison (NBCC 2010, ASCE 7-10, and EN 1991-4-1) of wind tunnel measurements on rectangular buildings with flat- and gabled-roofs. The paper examines the effect of building height, roof slope, and wind direction on wind load combinations; shear forces (in X- and Y- directions) occurring simultaneously with maximum torsion, as well as maximum shears and corresponding torsions.

2. Experimental Approach

The experiments were carried out in the boundary layer wind tunnel of Concordia University in Montreal, Canada. The working section of the tunnel is approximately 12.2 m long × 1.80 m wide. Its height is adjustable and ranging between 1.4 and 1.8 m to maintain negligible pressure gradient along the test section. A turntable of 1.2 m diameter is located on the test section of the tunnel and allows the testing of models for any wind direction. An automated Traversing Gear system provides the capability of probe placement to measure wind characteristics at any spatial location around a building model inside the test section. A geometric scale of 1:400 has been recommended for the simulation of the most important variables of the atmospheric boundary layer under strong wind conditions.

2.1. Building models

Figure 1 shows the two building models, with 0° and 45° gabled roof angles, equipped with 146 and 192 pressure taps on their surfaces, respectively. The flat roof does not have any pressure taps, since uplift forces do not contribute to torsion or horizontal shear forces. The models were tested at different building heights, by sliding them downwards in a precise tightly fit slot in the turntable, such that they can represent ten actual buildings with eave heights 20, 30, 40, 50 and 60 m. Model dimensions and the tested building heights are given in Table 1. In this study, all tested buildings were assumed to be structurally rigid and follow the limitations stated in the North-American and European wind codes/standards.

2.2. Terrain simulations

An open-country exposure was simulated in the wind tunnel. The flow approach profiles of mean wind velocity and turbulence intensity measured using a 4-hole Cobra probe (TFI) for the simulated terrain exposure (see Fig. 2). The wind velocity at free stream was 13.6 m/s. The power law index α of the mean wind velocity profile was set at $\alpha = 0.15$. Although it could be argued that it is not common for medium height buildings to be situated in open terrain, this exposure was chosen as a kind of conservatism since higher loads are expected to act on the tested buildings in this case. The pressure measurements on the models were conducted using a system of miniature pressure scanners from Scanivalve (ZOC33/64Px) and the digital service module DSM 3400. A standard tubing system was used in these measurements, in order to minimize the Gain and Phase shifts of pressure signals due to Helmholtz's resonance effects. Corrections were made by using traditional restrictors. The pressure measurement tubes have an outer and inner diameter of 2.18 and 1.37 mm respectively. The length is 55 cm and restrictors are installed at 30 cm from the location on the building model. All measurements were synchronized with a sampling rate of 300 Hz on each channel for a period of 27 sec (i.e., about one hour in full scale). It is well known that the mean wind speed has the tendency to remain relatively constant over smaller periods of time (i.e., 10 minutes to an hour) assuming stationarity of wind speed, as reported by van der Hoven (1957). This period is also suitable to capture the gust loads, which may be critical for structural design.

Table 1. Model dimensions and building heights tested

Building	Dimensions	
	Scaled @1:400 (mm)	Actual (m)
Width (B)	97.5	39
Length (L)	152.5	61
Tested heights (H)	50, 75, 100, 125, and 150	20, 30, 40, 50, and 60

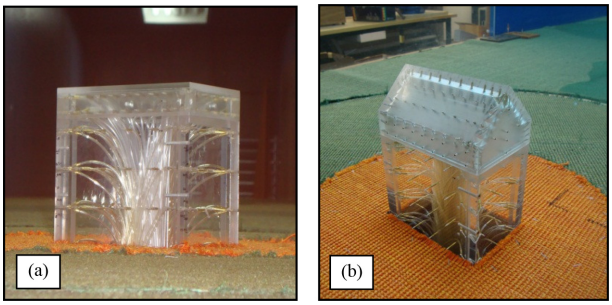


Figure 1. Wind tunnel models: (a) Building with a flat roof (0°); and (b) Building with a gabled roof (45°).

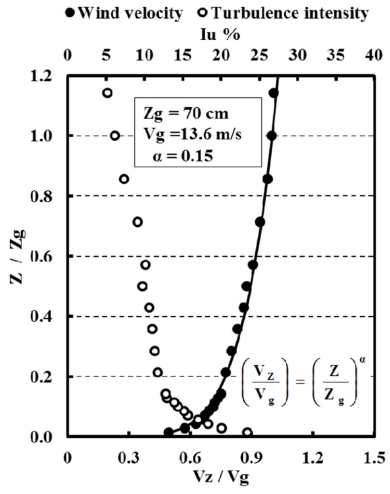


Figure 2. Wind velocity and turbulence intensity profiles for open terrain exposure.

3. Analytical Approach

Figure 3 shows a schematic representation of external pressure distributions on building envelope at a certain instant, the exerted shear forces, F_X and F_Y, along the two orthogonal axes of the buildings, as well as the torsional moment, M_T, at the geometric centre of the building. Pressure measurements are scanned simultaneously. The instantaneous wind force at each pressure tap is calculated according to:

$$f_{i,t}=p_{i,t}\times A_{effective} \quad f_{j,t}=p_{j,t}\times A_{effective} \tag{1}$$

Where $p_{i,t}$ and $p_{j,t}$ are instantaneous pressures measured at each pressure tap. The wind forces exerted at pressure tap locations in X- and Y-directions are noted by $f_{i,t}$ and $f_{j,t}$ respectively. For each wind direction, the horizontal force components in X- and Y-directions are evaluated according to:

$$F_X=\sum_{i=1}^{N} f_{i,t} \quad F_Y=\sum_{j=1}^{M} f_{j,t} \tag{2}$$

where N and M are the numbers of pressure taps on the longitudinal and transverse directions, respectively. All these forces are normalized with respect to the dynamic wind pressure at the roof height and the area as follows:

$$C_{sx}=\frac{F_X}{q_h B^2} \quad C_{sy}=\frac{F_Y}{q_h B^2} \tag{3}$$

where q_h = dynamic wind pressure (kN/m^2) at mean roof height h (m), B = smaller horizontal building dimension (m). The torsional coefficients C_T is evaluated based on:

$$C_T=\frac{M_T}{q_h B^2 L} \tag{4}$$

where L = larger horizontal building dimension

All peak shear and torsional coefficients ($C_{sx\,Max}$, $C_{sy\,Max}$, $C_{T\,Max}$) were considered as the average of the maximum ten values picked up from a 1-hr full-scale equivalent time history of the respective signal. This approach has been considered as a good approximation to the mode value of detailed extreme value analysis and it has been used in previous wind tunnel studies. The corresponding shear forces ($C_{sx\,corr.}$, $C_{sy\,corr.}$) and torsion ($C_{T\,corr.}$) were evaluated as the average of ten values occurring at the time instances of the ten peaks used to define the respective source maximum value. These corresponding shear/torsion values were normalized by the overall shear/torsion -evaluated as the most critical values found from testing the buildings for all wind directions, i.e., $C_{sx\,corr.}/C_{sx\,overall}$, $C_{sy\,corr.}/C_{sy\,overall}$, $C_{T\,corr.}/C_{T\,overall}$.

4. Experimental Results

4.1. Maximum torsion and corresponding shear forces in X- and Y-directions

As already mentioned, the two buildings with 0° and 45° gabled roof angles were tested in open terrain exposure at different eave heights (H = 20, 30, 40, 50 and 60 m) for different wind directions (0° to 90° every 15°). Figure 4(a) presents the variation of maximum torsion coefficient ($C_{T\,Max.}$) with wind directions for both building configurations and all tested heights. Figures 4(b) and 4(c) show corresponding shear ratios from the overall maximum shear forces in X- and Y-directions respectively (i.e., $C_{sx\,corr.}/C_{sx\,overall}$, $C_{sy\,corr.}/C_{sy\,overall}$). The maximum torsional coefficient increases significantly (about 2.5 times) with increasing building height from 20 to 60 m. The lowest torsional coefficient values occur when the wind direction is around 60°. Changing roof angle from 0° to 45° causes an increase of the torsional coefficient by about 50%. As expected,

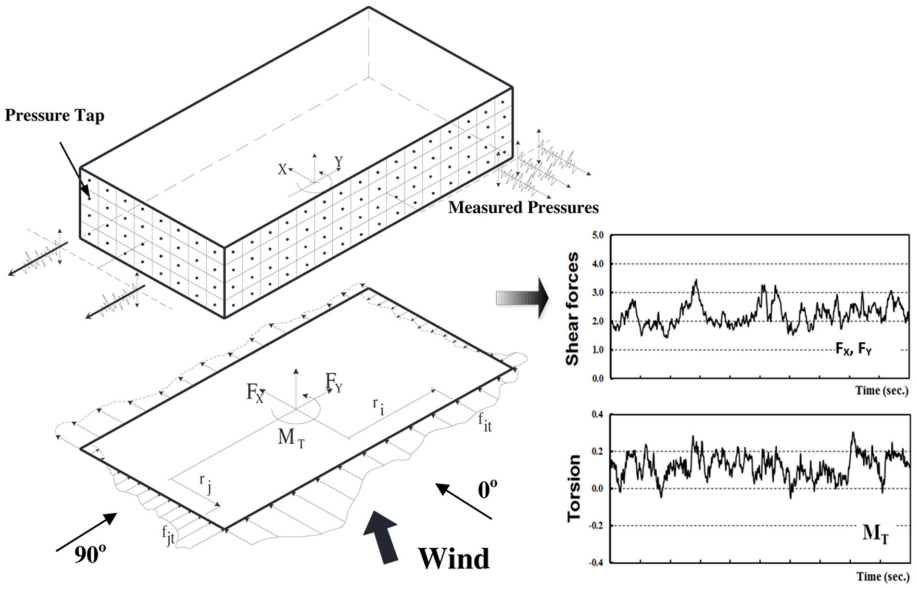


Figure 3. Measurement procedure for horizontal wind forces, F_X and F_Y, and torsional moment, M_T.

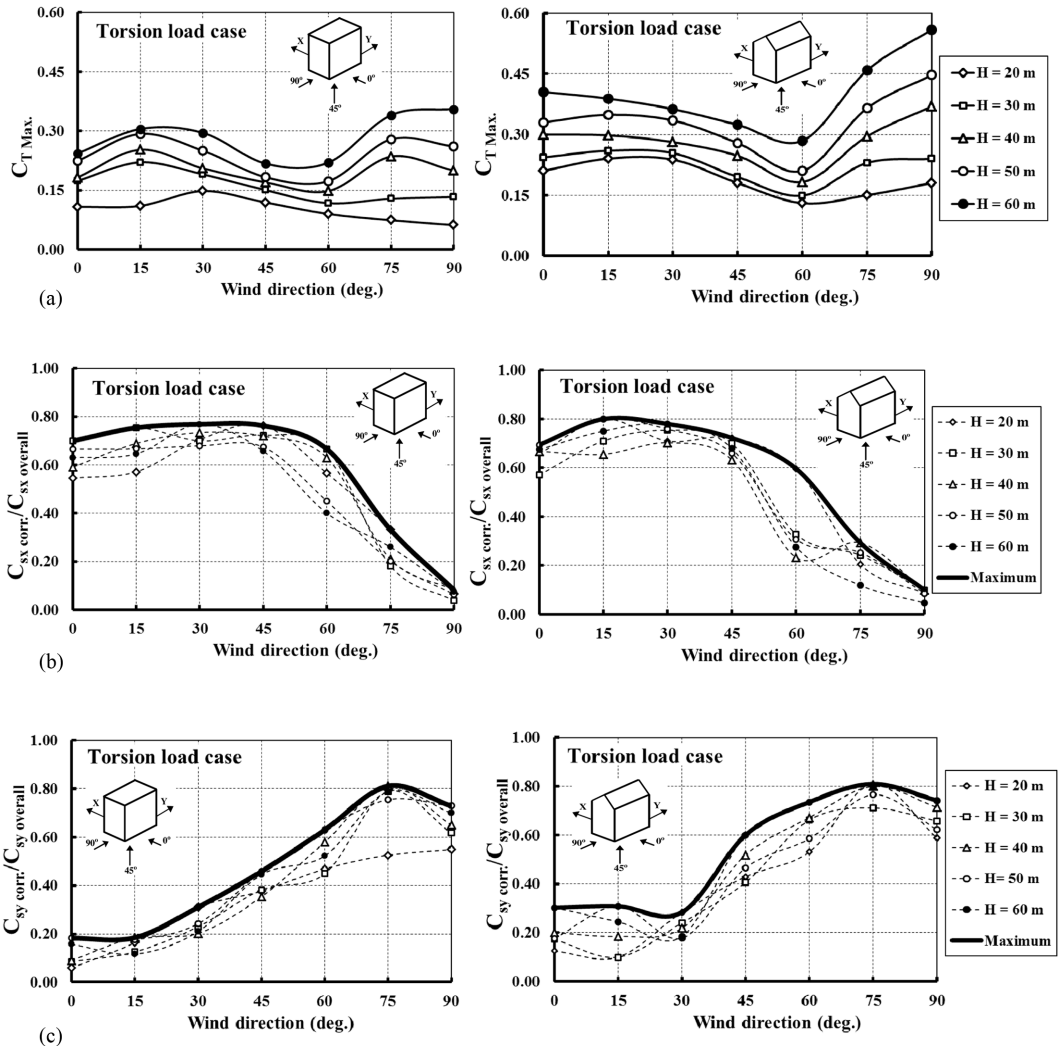


Figure 4. Torsion load case: (a) maximum torsion coefficient, (b) corresponding shear ratio in X-direction, (c) corresponding shear ratio in Y-direction.

the corresponding shear ratio in X-axis decreases when the incident wind angle varies from 0° to 90°. On the other hand, for the same wind range, the corresponding shear ratio in Y-axis increases. It is interesting to note that the maximum corresponding shear ratio is about 80% of the overall shear force for both X- and Y-directions, although for different wind directions. Moreover, the corresponding shear ratio has not been affected much by increasing building height or roof slope. The critical wind directions for torsion seem to be from 15° to 30° and 75° to 90°. In the first range, torsion is associated with higher shear force in X- than in Y-direction, while in the other range the higher shear force is in the Y-direction.

4.2. Maximum shear force in X-direction and corresponding torsion and shear force in Y-direction

Similarly, Fig. 5(a) presents the variation of the maximum shear force (X-component) evaluated for both building configurations and all tested heights for different wind directions. Figures 5(b) and 5(c) show the variation of corresponding torsion ratio ($C_{T\,corr.}/C_{T\,overall}$) and corresponding shear force ratio ($C_{sy\,corr.}/C_{sy\,overall}$) with wind direction, respectively. Maximum shear force coefficient ($C_{sx\,Max.}$) has increased significantly (almost triple and double for flat- and gabled-roof) by increasing the height of the building from 20 to 60 m. Changing roof angle from 0° to 45° results in increasing shear force coefficient ($C_{sx\,Max.}$) by about 2.4 times for the 20 m building and 1.5 times for the 60 m building. This may be attributed to the reduction of the ratio of the inclined roof area facing the wind relative to the total surface building area resulting from increasing building height from 20 to 60 m. Thus, it is clear that the effect of increasing roof slope on the maximum shear force decreases with increasing building height. The maximum shear coefficient in X-direction has not been affected much by changing the wind direction from 0° to 45° while rapid decrease was noted from 45° to 90°. The corresponding torsion ratio tends to reach its peak value for wind directions between 15° and 30° for the two tested buildings at different heights. On the other hand, the corresponding

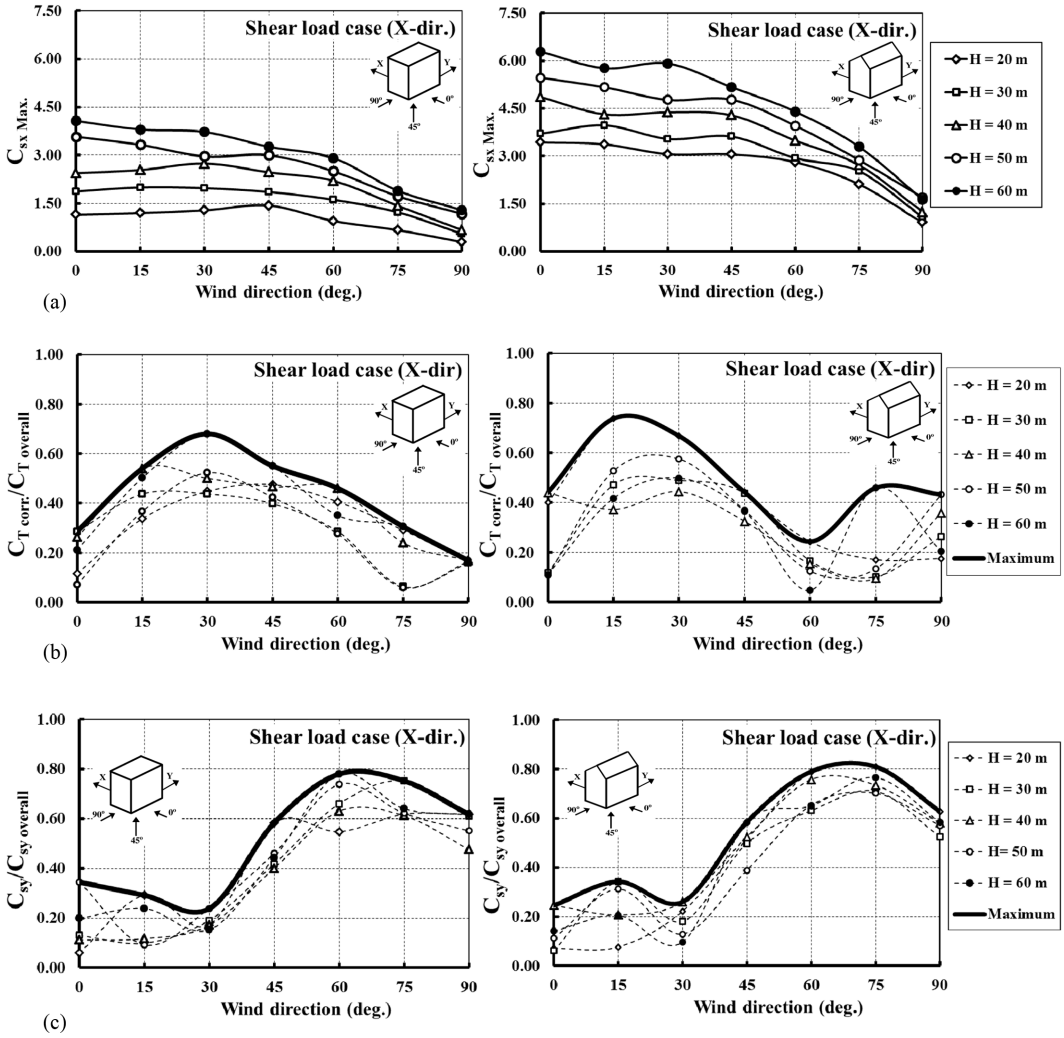


Figure 5. Shear load case (transverse direction): (a) maximum shear coefficient in X-direction, (b) corresponding torsion ratio, (c) corresponding shear ratio in Y-direction.

shear force ratio ($C_{sy\ corr.}/C_{sy\ overall}$) seems to be lower when wind directions are between 0° and 45° and higher between 45° and 90°. The peak corresponding shear force ratio ($C_{sy\ corr.}/C_{sy\ overall}$) was reported for a wind direction between 60° and 75° as 80%. The shear load case in transverse direction should account for the maximum shear force in X-direction, the corresponding torsion, and the corresponding shear in Y-direction for wind directions from 0° to 45°. However, for wind directions ranging from 45° to 90°, the shear in Y-direction will be maximized and this will be more critical for designing the building in the longitudinal direction, as it will be illustrated in the following sections.

4.3. Maximum shear force in Y-direction and corresponding torsion and shear force in X-direction

Figure 6(a) presents the variation of the maximum shear force in Y-direction evaluated for different wind directions for the same building configurations. Also, Figures 6(b) and 6(c) show the variation of corresponding torsion ratio ($C_{T\,corr.}/C_{T\,overall}$) and corresponding shear force ratio ($C_{sx\ corr.}/C_{sx\ overall}$) with wind direction, respectively. Similar to the shear force in X-direction, the maximum shear force coefficient ($C_{sy\ Max.}$) has increased significantly (about 2.8 times) by increasing the height of the flat-roofed building from 20 to 60 m and by about 1.8 times for the gabled-roof (45°) building. Changing roof angle from 0° to 45° results in almost doubling the shear force coefficient ($C_{sy\ Max.}$) for the 20 m high building but in only 30% increase for the 60 m high building. The maximum shear coefficient in Y-direction has not been affected much by changing the wind direction from 45° to 90°. Accordingly, the corresponding torsion ratio reaches its peak value at wind direction of 75° for the two tested buildings at different heights. The corresponding shear force ratio ($C_{sx\ corr.}/C_{sx\ overall}$) seems to be lower for wind directions from 45° to 90°. The peak corresponding shear force ratio ($C_{sx\ corr.}/C_{sx\ overall}$) was found to be 0.8 for 0° wind direction. Although the effects of increasing roof slope from 0° to 45° lead to increasing the maximum torsion and shear forces for different wind directions - as mentioned earlier - the corresponding component

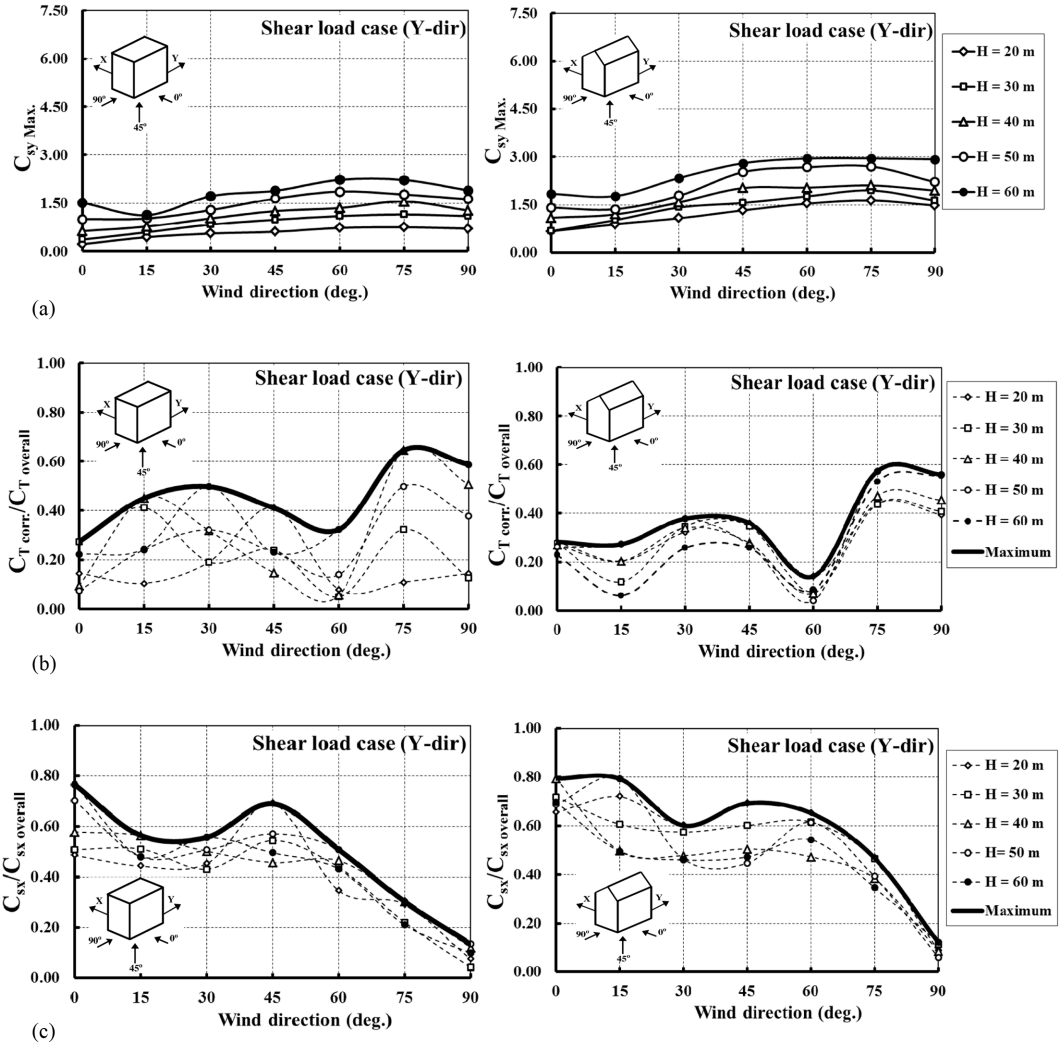


Figure 6. Shear load case (longitudinal direction): (a) maximum shear coefficient in Y-direction, (b) corresponding torsion ratio, (c) corresponding shear ratio in Y-direction.

ratios are similar for flat-roofed and gabled-roofed buildings. Likewise, the shear load case in longitudinal direction should account for the maximum shear force in Y-direction, the corresponding torsion, and the corresponding shear ratio in X-direction for winds in the range of 45° to 90°.

5. Comparison with Previous Studies

A comparison of the results with those from a previous study by Isyumov and Poole (1983) for a building with dimensions $L = 91.45 \times B = 45.7 \times H = 231.65$ m and a more recent study from Keast et al. (2012) for a building with dimensions $L = 40 \times B = 20 \times H = 60$ m was made using the wind tunnel measurements in the current study for a modeled full-scale building with $L = 61 \times B = 39$ m $\times H = 60$ m. As the building tested by Isyumov and Poole 1983 was very tall and the power law index (α) for actual exposure was also not specified, the mean torsion evaluated for different wind directions was only considered for this comparison. For the case of Keast et al. (2012), the building dimensions and the terrain exposure were similar, therefore a complete comparison was carried out. Past studies have used shear and torsional coefficients defined as; C_v = Base shear/(q_H LH) and C_T = Base torsion/(q_H L^2H), respectively, where q_H = dynamic wind pressure at mean roof height, L = larger horizontal building dimension. For comparison purposes, the results of the current study have been transformed to the same definitions of shear and torsional coefficients. Table 2 presents the experimental parameters as well as the evaluated shear and torsional coefficients for the buildings considered. Figure 7 shows good agreement of the mean torsional coefficients for different wind directions evaluated by the three studies; and the peak torsional coefficients of the present study with those by Keast et al. (2012). Furthermore, Fig. 8 presents the ten most critical torsion values recorded from all wind directions along with the corresponding shear force ratio measured by Keast et al. (2012) and the respective values from the current study. Results show relatively good agreement for the measured shear forces and torsion in the two

Table 2. Comparison with Isyumov and Poole (1983) and Keast et al. (2012)

	Isyumov and Poole (1983)	Keast et al. (2012)	Current study
Wind tunnel technique	Weighted pneumatic averaging	A 6 degree-of-freedom high frequency balance	High frequency pressure integration
Building dimensions (m)	L=91.45 × B=45.7 × H=231.65	L=40 × B=20 × H=60	L=61 × B=39 × H=60
Aspect ratio (L/B)	2	2	1.60
Scale	1:500	1:400	1:400
Model dimensions (mm)	182.9 × 91.4 × 463.3	100 × 50 × 150	152.5 × 97.5 × 150
Terrain exposures	Suburban	Open	Open (α = 0.15)
Wind direction	0° to 90°	0° to 90°	0° to 90°
Torsional coeff. ($C_{T\,max}$)	N/A	0.14	0.15
Shear coefficient ($C_{vx\,max}$)	N/A	2.00	1.80
Shear coefficient ($C_{vy\,max}$)	N/A	0.75	0.90

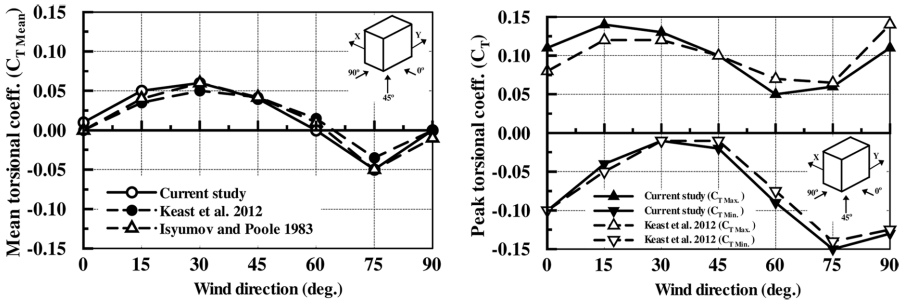


Figure 7. Torsional coefficient comparison for flat-roofed rectangular buildings with height 60 m located in open country exposure.

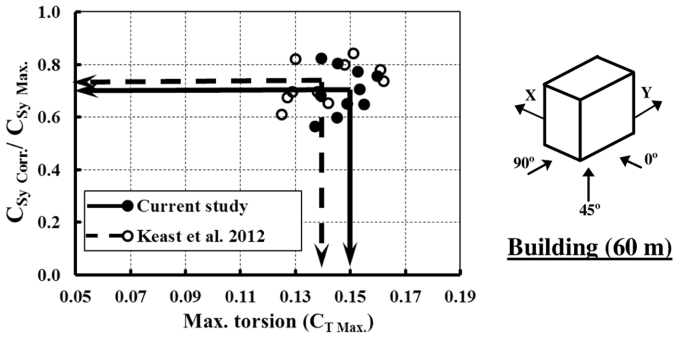


Figure 8. Overall shear ratios ($C_{sy\,Corr.}/C_{sy\,Max.}$) at peak torsion for the 60 m high flat-roofed building evaluated by Keast et al. (2012) and those from current study.

studies. Small differences could be attributed to the difference in building dimensions, the scale used, and the number of pressure taps.

Another comparison with a previous study by Tamura et al. (2003) for a building with dimensions L = 50 m × B = 25 m × H = 50 m was made using a building model having L = 61 m × B = 39 m × H = 50 m. The two flat-roofed buildings have the same height and aspect ratios of their plan dimensions L/B = 2 and 1.6. In this comparison, the definitions of torsional and shear coefficients in the Tamura et al. (2003) study were followed. The torsional coefficient was considered as C_T = Base torsion/(q_H LHR) where; R = (L^2 + B^2)/2, B = smaller horizontal building dimension, and shear coefficient C_v = Base shear/(q_H LH). Tamura et al. (2003) study shows higher coefficients by about 60% (see Table 3), but this may be attributed to the different terrain exposures used in these studies. Indeed, the mean wind velocity at the roof height in urban terrain is much lower than that in open terrain exposure.

6. Comparisons of Experimental Results with Code Provisions

It is also quite interesting to compare the wind tunnel results with wind load provisions in the current codes and standards. Three sets of wind load provisions were chosen for the comparison, namely; National Building Code of Canada (NBCC, 2010), American Society of Civil Engi-

Table 3. Comparison with previous study by Tamura et al. (2003)

Experimental variables	Tamura et al. (2003)	Current study
Wind tunnel technique	High frequency pressure integration	High frequency pressure integration
Building dimensions (m)	L=50 × B=25 × h=50	L=61 × B=39 × h=50
Aspect ratio (L/B)	2.0	1. 6
Scale	1:250	1:400
Model dimensions (mm)	200 × 100 × 200	152.5 × 97.5 × 125
Terrain exposures	Urban (α = 0.25)	Open (α = 0.15)
Wind direction	$\perp$ to building length (L=50 m)	$\perp$ to building length (L=61 m)
Torsional coefficient ($C_{T\,max}$)	0.30	0.20
Shear coefficient ($C_{vx\,max}$)	3.00	1.90
Shear coefficient ($C_{vy\,max}$)	0.90	0.50

neers Standard (ASCE 7-10), and European Building Code (EN 1991-4-1).

NBCC 2010 requires for design of medium-rise buildings to apply 50% of the full wind load (P) on half of the along wind wall in order to predict the maximum torsion. On the other hand, ASCE 7-10 requires introducing 75% of the full wind load with eccentricity of 15% of the perpendicular building dimension for evaluating maximum torsion. The non-uniform distribution of wind loads were simulated by applying triangular load in the EN 1991-1-4. Figure 9 compares torsional load cases specified for designing of medium-rise buildings in the three wind codes/ standards.

The external pressure by the simplified method (NBCC, 2010) is taken from figure I-16, Commentary I, and the gust factor (Cg) was taken as 2. The partial load case was implemented by completely removing the full wind loads from half of building faces to estimate maximum torsion and corresponding shear as specified in Case B in figure I-16, Commentary I. The directional-part I method (ASCE 7-10) assigned for enclosed, partially enclosed, and open buildings of all heights was applied. The side wall external pressure coefficient (Cp) was estimated according to figure 27.4-1. Open terrain exposure C was considered, with the directional factor (Kd) and the gust factor (G) taken as 1 and 0.85, respectively. Maximum torsion and corresponding shear were estimated by applying 75% of the full wind load and equivalent eccentricity of 15% of building width, as indicated in Case 2 in figure 27.4-8. Similarly, for EN 1991-1-4 (2005), the external pressure coefficients for vertical walls of rectangular plan buildings are calculated using

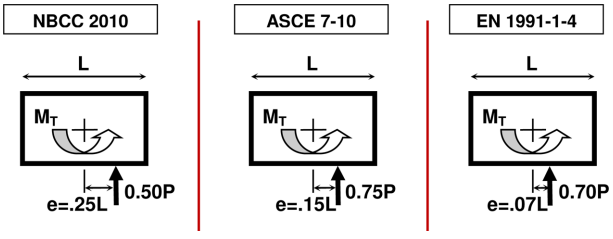


Figure 9. Comparison of the torsional load cases specified for medium-rise buildings in NBCC 2010, ASCE 7-10 and EN 1991-1-4.

figure 7.5 and table 7.1 available in section 7. The non-uniform distribution of wind loads was recognized by applying triangular loading (EN 1991-1-4, 2005).

For the evaluation of the maximum shear force, NBCC 2010, ASCE 7-10 and EN 1991-4-1 apply the full wind load on building face uniformly but neglect completely the associated torsion. All ASCE 7-10 values were multiplied by 1.51^2 and EN 1991-1-4 values by 1.06^2 in order to consider the effect of the 3-sec and the 10-min wind speed respectively in comparison to the mean-hourly wind speed in NBCC 2010. The shear coefficient and torsional coefficient were estimated by using Eqs. 3 and 4.

Figure 10 summarizes the results for shear load case evaluated by the three code provisions and the wind tunnel in transverse and longitudinal directions. Clearly, the three building codes and standards overestimate shear force on medium-rise buildings for both directions. This may be a kind of compromising to compensate for neglecting the corresponding torsion, which may not be always critical in design situations. Figure 11 shows the comparison for the torsional load case. Clearly NBCC 2010 and ASCE 7-10 overestimate torsion significantly on the tested building in the transverse direction but results compare better in the longitudinal direction. The EN 1991-4-1 compares well with the wind tunnel in transverse direction but underestimates torsion significantly in the longitudinal direction.

7. Suggested Wind Load Combination Factors for Design of Rectangular Buildings

Table 4 summarizes the peak torsion ($C_{T\,Max.}$) and shear force coefficients ($C_{sx\,Max.}$, $C_{sy\,Max.}$) evaluated by the wind tunnel for the two buildings tested at all heights in open terrain exposure. Tables 5 and 6 present the corresponding wind force component ratios obtained from testing the two buildings with flat-roof (0°) and gabled-roof (45°) respectively, for all wind directions. The corresponding wind force component ratios reported in Tables 5 and 6 are the highest ratios obtained from testing all building heights, hence they are conservative. These values are associated to the peak torsion, peak shear force in X-direction, and peak shear force in Y-direction respectively.

Based on the wind tunnel results, Table 7 presents the

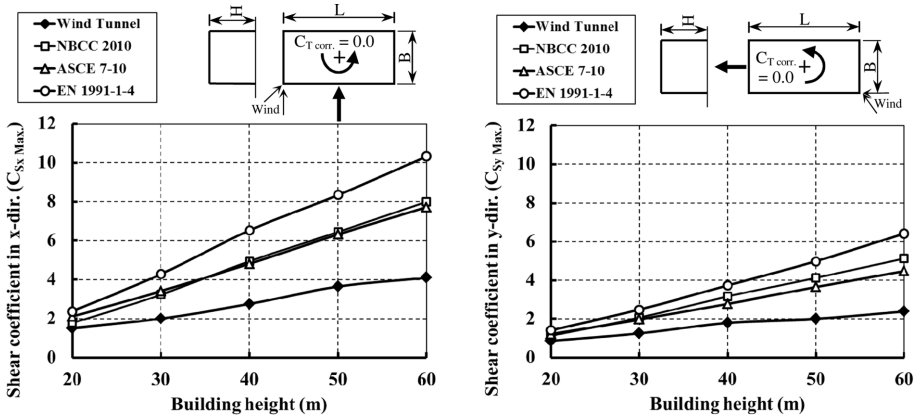


Figure 10. Comparison of peak shear coefficients ($C_{sx\,Max.}$ and $C_{sy\,Max.}$) evaluated by wind tunnel, NBCC2010, ASCE7-10, and EN 1991-1-4.

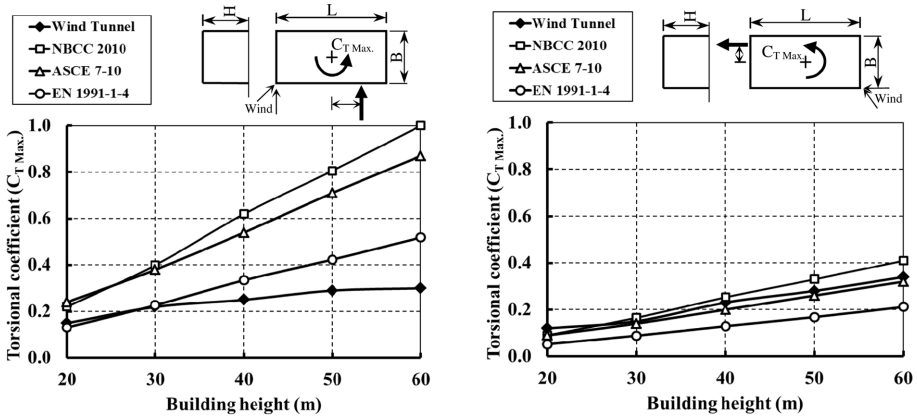


Figure 11. Comparison of peak torsion coefficient ($C_{T\,Max.}$) evaluated by wind tunnel, NBCC2010, ASCE7-10, and EN 1991-1-4.

Table 4. Peak torsion and shear force coefficients evaluated from all wind directions

Building height (m)	Flat-roof (0°)			Gabled-roof (45°)		
	$C_{T\,Max.}$	$C_{sx\,Max.}$	$C_{sy\,Max.}$	$C_{T\,Max.}$	$C_{sx\,Max.}$	$C_{sy\,Max.}$
20	0.15	1.45	0.80	0.24	3.43	1.63
30	0.22	2.00	1.20	0.26	3.97	1.94
40	0.25	2.75	1.60	0.37	4.86	2.10
50	0.30	3.60	1.90	0.45	5.47	2.70
60	0.36	4.10	2.25	0.56	6.29	2.96

suggested wind load combination factors for designing medium-rise buildings with rectangular plan. Shear and torsion load cases are provided for transverse and longitudinal directions, as illustrated in Fig. 12. The shear load case in transverse direction was defined by applying the maximum shear force in X-direction (given in Table 4) with the corresponding torsion and shear in Y-direction. These corresponding values were introduced in a form of ratio from the maximum torsion or shear component and this ratio is the highest obtained from testing the two buildings in wind direction range 0° to 45°. For instance, the highest corresponding torsion ratio due to winds in transverse direction - wind direction range 0° to 45° - for the flat- and gabled-roof buildings are 0.68, 0.74, see Tables 5 and 6. As indicated in Table 7 the corresponding torsion will be 0.75 (rounded number from 0.74) of the maximum torsion (given in Table 4). Likewise, the torsion load case in the transverse direction was defined by applying the maximum torsion and the corresponding shear forces in X- and Y-directions obtained for wind directions between 0° and 45°.

Furthermore, in longitudinal direction the shear and torsional load case were defined as the maximum shear force in Y-direction and maximum torsion with the corresponding values resulting from testing the building in wind directions ranging from 45° to 90°.

Table 5. Peak corresponding force component ratios for building with flat-roof (0°) tested at all heights

	Wind direction (deg.)						
	0	15	30	45	60	75	90
Torsional load case:							
$C_{sx\ corr./overall}$	0.70	0.75	0.77	0.76	0.67	0.33	0.08
$C_{sy\ corr./overall}$	0.18	0.18	0.31	0.46	0.63	0.81	0.73
Shear load case (X-direction):							
$C_{T\ corr./overall}$	0.29	0.54	0.68	0.55	0.46	0.31	0.17
$C_{sy\ corr./overall}$	0.34	0.29	0.24	0.58	0.78	0.75	0.62
Shear load case (Y-direction):							
$C_{T\ corr./overall}$	0.27	0.45	0.50	0.41	0.32	0.64	0.59
$C_{sx\ corr./overall}$	0.77	0.56	0.56	0.69	0.51	0.30	0.13

Table 6. Peak corresponding force component ratios for building with gabled-roof (45°) tested at all heights

	Wind direction (deg.)						
	0	15	30	45	60	75	90
Torsional load case:							
$C_{sx\ corr./overall}$	0.69	0.80	0.78	0.72	0.60	0.29	0.10
$C_{sy\ corr./overall}$	0.30	0.31	0.28	0.60	0.74	0.81	0.74
Shear load case (X-direction):							
$C_{T\ corr./overall}$	0.44	0.74	0.67	0.44	0.24	0.46	0.43
$C_{sy\ corr./overall}$	0.25	0.34	0.26	0.58	0.79	0.81	0.63
Shear load case (Y-direction):							
$C_{T\ corr./overall}$	0.28	0.27	0.38	0.36	0.14	0.57	0.56
$C_{sx\ corr./overall}$	0.79	0.79	0.60	0.69	0.65	0.47	0.12

Table 7. Suggested design load combination factors for rectangular buildings

	Load case	C_T*	C_{sx}*	C_{sy}*
Transverse direction	Shear	0.75	1	0.60
	Torsion	1	0.80	0.60
Longitudinal direction	Shear	0.65	0.70	1
	Torsion	1	0.35	0.80

(*These values are the absolute maximum coefficients for each load case. Refer to Tables 4, 5 and 6 for simultaneous and maximum values for the flat- and gable-roofed rectangular buildings.)

Naturally, additional experimental work for buildings with different aspect ratios would be useful in order to generalize the current findings.

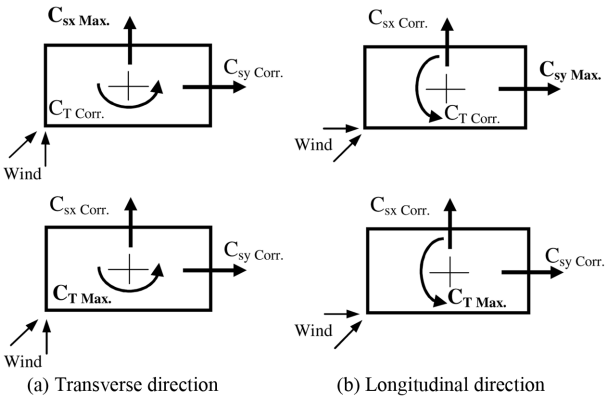


Figure 12. Suggested shear and torsion wind load cases in transverse and longitudinal directions for rectangular building design.

8. Conclusions

Shear and torsional design wind load cases were investigated in a boundary layer wind tunnel for rectangular, flat and gable-roofed medium-rise buildings in open terrain exposure. The results show that maximum torsion for winds in the transverse direction is associated with 80% of the overall shear force perpendicular to the largest building horizontal dimension and 60% of the maximum shear force perpendicular to the smallest building horizontal dimension, while for winds in the longitudinal direction maximum torsion is associated with 80% and 35% of the maximum shear perpendicular to the smallest and largest dimensions respectively. Furthermore, comparisons of the experimental results with the NBCC 2010, ASCE 7-10, and EN 1991-4-1 provisions show that these codes generally overestimate maximum shear force in transverse and longitudinal directions but they neglect the associated torsion. NBCC 2010 and ASCE 7-10 overestimate maximum torsion for winds in the transverse direction while comparable values were found for winds in the longitudinal direction. Finally, EN 1991-4-1 underestimates torsion for winds in the longitudinal direction but compares well with the experimental data in the transverse direction. Suggested wind load combination factors are presented to account for maximum shear along with associated torsion and maximum

torsion along with associated shear.

References

ASCE 7. (2010). "Minimum design loads for buildings and other structures." Structural Engineering Institute of ASCE, Reston, VA.

CEN. (2005). "Eurocode 1: Actions on Structures - Part 1-4: General actions - Wind actions." *Pr EN 1991-1-4*, Brussels.

Elsharawy, M., Stathopoulos, T. and Galal, K. (2012). "Wind-Induced torsional loads on low buildings." *Journal of Wind Engineering and Industrial Aerodynamics*, 104-106, pp. 40~48.

Elsharawy, M., Galal, K. and Stathopoulos, T. (2013). "Comparison of wind tunnel measurements with NBCC 2010 wind-induced torsion provisions for low- and medium-rise buildings." *Canadian Journal of Civil Engineering*, Submitted.

Isyumov and Poole. (1983). "Wind induced torque on square and rectangular building shapes." *Journal of Wind Engineering and Industrial Aerodynamics,* 13(1-3), pp. 183~196.

Keast, D. C., Barbagallo, A. and Wood, G. S. (2012). "Correlation of wind load combinations including torsion on medium-rise buildings." *Wind and Structures, An International Journal*, 15(5), pp. 423~439.

NBCC. (2010). "User's Guide - NBC 2010, Structural Commentaries (part 4)." Issued by the Canadian Commission on Buildings and Fire Codes, National Research Council of Canada.

Sanni, R. A., Surry, D. and Davenport, A. G. (1992). "Wind loading on intermediate height buildings." *Canadian Journal of Civil Engineering*, 19, pp. 148~163.

Stathopoulos, T. and Dumitrescu-Brulotte, M. (1989). "Design recommendations for wind loading on buildings of intermediate height." *Canadian Journal of Civil Engineering*, 16, pp. 910~916.

Tamura, Y., Kikuchi, H. and Hibi, K. (2003). "Quasi-static wind load combinations for low- and middle-rise buildings." *Journal of Wind Engineering and Industrial Aerodynamics*, 91, pp. 1613~1625.

Tamura, Y., Kikuchi, H. and Hibi, K. (2008). "Peak normal stresses and effects of wind direction on wind load combinations for medium-rise buildings." *Journal of Wind Engineering and Industrial Aerodynamics*, 96(6-7), pp. 1043~1057.

Van der Hoven, I. (1957) "Power spectrum of wind velocities fluctuations in the frequency range from 0.0007 to 900 Cycles per hour." *Journal of Meteorology*, 14, pp. 160~164.